

A STUDY OF ON-ORBIT BEHAVIOUR OF InGaAs SWIR CHANNEL DEVICE OF IRS-1C/1D LISS-III CAMERA

A.S Kirankumar, P.N Babu and R.Bisht

Sensor Systems Division, Space Applications Centre, Ahmedabad-380053

Abstract - The Indian Remote Sensing Satellite (IRS-1C), at an altitude of 817 Km, completed two years of operation in space on December 25, 1997. The multi-spectral LISS-3 push-broom camera in IRS-1C has a 1.55-1.70 μm wavelength range Short-Wave Infra-Red (SWIR) spectral band providing imagery at 70 metres ground resolution to cover various remote sensing applications. This band is realised through a state of the art technology Indium Gallium Arsenide photo-diode linear array, the first of its kind in space. The device consists of lattice mismatched hetero-junction photo-diode array for sensing the radiation and the signal is readout by the Silicon based CCD multiplexers. The device is operated at -10°C with tight temperature control necessary to contain the dark current signal fluctuations. The device temperature requirements are realised through a passive radiative cooler and an on-off heater control. The camera has In-Flight Calibration Unit which is realised through four SWIR light emitting diodes operated in pulsed mode to generate six intensity levels. The unique features of this calibration scheme enable the study of various device parameters like responsivity, linearity, darksignal, etc.,. The paper describes the results of a study conducted over the time utilising the periodically collected in-flight calibration data.

1. INTRODUCTION

Remote sensing from satellite platforms has provided a unique opportunity to study properties of the Earth and to monitor its resources. 1.55 to 1.70 μm Short Wave Infrared (SWIR) spectral wavelength band plays an important role in monitoring vegetation, water resources, and to study the surface composition of Earth.

Indian Remote Sensing Satellites, IRS-1C/1D, carry SWIR wavelength band as part of their multi-spectral LISS-III push-broom camera. This SWIR channel provides a ground spatial resolution of 70 meters with a swath of 148 Kms. The incorporation of this channel was possible because of the availability of near-room temperature operated linear array of InGaAs photo-diodes developed by THOMSON-CSF, France.

2. THE SWIR DEVICES

The device is built with seven identical elementary modules mechanically butted together and enclosed in a ceramic package with glass window to form the required array of 2100 pixels in a single line. Each elementary module consists of two-side buttable InGaAs die of 300 photo-diodes and two 150 element Silicon based CCD arrays on either side of the photo-diode die to multiplex the signal from the photo-diodes. The photo-sensitive photo-diode of $\text{In}(x)\text{Ga}(1-x)\text{As}$ is grown on Indium Phosphide (InP) substrate followed with an InP cap layer to form a double hetero-junction InGaAs photo-diodes. Lattice-matched InGaAs over InP would correspond to the bandgap energy leading to 1.67 μm cut-off wavelength. In order to extend the cut-off wavelength beyond 1.7 μm , a lattice mismatch of 3% is introduced between InGaAs and InP. Further, the photo-diodes are reverse-biased and the device works in vidicon mode i.e. the photo-generated holes (electrons are grounded) reduce the reverse-bias of the diode and a fraction of known amount of electrons (pre-load), which are channelled into the diode, restore this reverse-bias; the remaining electrons are collected back as inverted photo signal.

In case of IRS-1C, the photo-diodes with photo-sensitive area (pixels) of $30\mu\text{m} \times 30\mu\text{m}$ each are arranged with 26 μm pitch and staggered in two rows, 52 μm centre to centre. The SWIR device of IRS-1D is similar except it has an in-line pixel arrangement with $20\mu\text{m} \times 30\mu\text{m}$ pixel size. The positional accuracy of pixels in both devices is $\pm 1\mu\text{m}$ to permit very good pixel to pixel registration with the other three wavelength bands of LISS-III camera.

3. ONBOARD OPERATING TEMPERATURE

In order to achieve a radiometric resolution of 7 bits, to reduce the dark noise to less than $\pm \frac{1}{2}$ bit and to reduce the number of non-usable pixels due to high dark signal below acceptable limits, SWIR device of IRS-1C has to be operated at a controlled low temperature. Table 3.1 shows the number of non-usable pixels at different temperatures for three such SWIR devices. It can be seen from this table that the number of non-usable pixels reduce drastically as the temperature of the devices is reduced to -10°C . Thus, the SWIR device of IRS-1C is being operated onboard at $-10 \pm 0.15^\circ\text{C}$ (provision exists to operate the device at $-5 \pm 0.15^\circ\text{C}$ also). Because of the improved technology used for fabrication of IRS-1D SWIR device, it is being operated onboard at a controlled (within $\pm 0.15^\circ\text{C}$) temperature of 12°C with a provision for 15°C operation. In comparison to the Electro-Optical Module (consisting imaging optics, detector head assembly and detector electronics and mechanical housing) temperature of $20 \pm 3^\circ\text{C}$, the lower temperature operation of the SWIR devices is realised by using copper braids to conduct away the heat from detector area, which is thermally well isolated from the detector head assembly and the rest of the EOM, to a cold radiator plate mounted on the satellite deck. A thermistor and a thermo-foil heater in closed loop is used to control the temperature within $\pm 0.15^\circ\text{C}$. Table 3.2 gives the radiator plate as well as detector operating temperature achieved onboard for IRS-1C SWIR device during various orbits from January 1996 to February 1997.

Table 3.1
Non-Usable Pixels versus device temperature

Device temperature (°C)	Number of non-usable pixels with the three available detectors for IRS-1C		
	1	2	3
23	288	451	285
20	249	278	179
17	202	216	217
10	126	136	71
5	92	105	46
0	79	96	43
-5	73	77	40
-10	68	72	40

Table 3.2
SWIR detector temperature variation in IRS-1C

Orbit No.	Temperature in Degrees Centigrade	
	Radiator Plate (±0.5)	Detector (±0.25)
56	-30 to -35	-10
511	-31 to -36	-10
923	-30 to -36	-10
1349	-30 to -36	-10
1790	-30 to -34	-10
2216	-27 to -34	-10
2642	-29 to -36	-10
3097	-30 to -34	-10
3523	-30 to -34	-10
3963	-28 to -34	-10
4390	-28 to -34	-10
4816	-30 to -34	-10
5271	-27 to -34	-10
5697	-30 to -36	-10
5896	-30 to -36	-10

4. ONBOARD CALIBRATION UNIT

Provision has been made for on-board calibration of the SWIR device with 1.55 μm Infra-red light emitting diodes as illuminating source. The in-flight calibration unit is comprised of two sets of IR LEDs, one on either side of the photo-diode array. Each LED is followed by a diverging optics. One calibration cycle consists of 2048 scan lines and includes six intensity levels (I1 to I6) plus dark (no illumination) level (Io) as defined in Table 4.1.

The LEDs are operated in pulse mode with two exposure levels (5.4 ms exposure time for I1 to I3 and 10.8 ms for I4 to I6). Two consecutive intensity levels are separated by seven dark scan lines. This calibration provision, utilised during the night satellite passes, enables regular

evaluation of the performance of the device with time. Based on an analysis of on-board calibration data and a comparison with ground performance, the on-board performance of the device is studied.

TABLE 4.1
Details of the In-flight Calibration Cycle

Intensity level	Definition	Number of occurrences in one cycle
I1	Set 1 on, Set 2 off	43
I2	Set 1 off, Set 2 on	42
I3	Both sets on	42
I4	Set 1 on, Set 2 off	43
I5	Set 1 off, Set 2 on	42
I6	Both sets on	42
Io	No illumination	1794

5. NON-USABLE PIXELS

Due to the mechanical butting of the elementary modules, one pixel at each splice is non-usable. Thus, seven pixels are non-responsive due to the device manufacturing technology. Apart from these, there could be more non responsive pixels due to missing wire bonds between photo-diodes and the CCD multiplexers (manufacturing defect).

Further, the device could have saturated response pixels (output of these pixels always saturates the channel output). Pixels can also be non-usable because of their high dark signal or high standard deviation (noisy pixels) causing low signal to noise ratio. Thus, a device can have four different categories of non-usable pixels. Table 5.1 show these non-usable pixels for SWIR devices used in IRS-1C and IRS-1D spacecraft.

TABLE 5.1
Non-usable pixels of SWIR devices of IRS-1C/1D

Type	Pixel Class	Number of Pixels	
		IRS-1C	IRS-1D
1	Non-Responsive	14	7
2	Saturated	14	0
3	High Dark Signal	5	1
4	High Standard Deviation	7	0

6. ON-BOARD PERFORMANCE

IRS-1C satellite was launched in December, 1995 and IRS-1D in September 1997. SWIR channel data for both the satellites are regularly being collected since their respective launch. The calibration mode of operation of the SWIR channel is regularly being carried out. Calibration data used for the present study are from January 1996 to December 1996 and one orbit data of January 1998 in case of

IRS-1C; and October 1997 and January 1998 data in case of IRS-1D.

6.1 Dark Signal

In order to see the individual pixel dark signal variation with time, the dark signal for each pixel is obtained from calibration data and averaged over eight scan lines in each calibration cycle of an orbit. The dark signal is also averaged for odd and even channels (150 pixels each) of all seven modules for different orbits; this is to see channel wise behaviour of dark signal. Each intensity level (I1 to I6) data for each pixel is averaged over 42 scan lines of the calibration cycle and its value for different orbits is used to study the temporal change in the response of individual pixels. Further, even and odd channel wise average of these illuminated data are also obtained to study the temporal behaviour of each channel under illuminated conditions.

Table 6.1 shows the module-wise channel-wise average dark signal and illuminated (I1 to I6) signal for different orbits in case of SWIR device of IRS-1C satellite. It can be seen from this table that the average dark signal of each channel does not show any increase with time.

The dark signal data for individual pixels show that in case of SWIR devices of both the satellites some pixels have developed high dark signal during onboard operation of the devices and the number of such pixels is increasing with time. It is very important to note from Fig.6.2, showing a typical observed change pattern of dark signal, that the increase in dark signal of these pixels is abrupt.

In case of IRS-1C, since January 1996 to December 1997, the dark signal of 47 pixels increased by more than two counts and this number has increased to 95 by January 1998. Module wise distribution of these affected pixels (Table 6.2) shows that the distribution of affected pixels among different modules is similar and the affected pixels do not show any preference towards any particular module.

Table 6.2

Modulewise Development of Dark signal pixels

Elementary Module	IRS-1C upto		IRS-1D
	Jan'97	Jan'98	(over 4 months)
1	9	15	1
2	5	13	4
3	6	13	2
4	4	13	0
5	6	13	2
6	8	13	0
7	9	15	2
Total	47	95	11
Pixels per month	3.8		2.7

The dark signal behaviour of these pixels with time (for different orbits) is shown in Table 6.3 for a few. In addition, a monotonic increase is evident in the cumulative

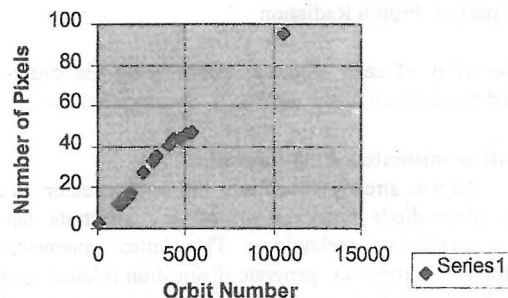
number of dark signal development pixels with time (Fig. 6.1).

Table 6.3

Dark signal developed pixel behaviour with time

Orbit Number	Dark signal of pixel no.1635 in camera counts			
	Min.	Mean	Max.	Standard deviation
121	0	0.0	0	0.0
1825	0	0.0	0	0.0
1897	0	0.0	0	0.0
2649	15	15.0	15	0.0
3175	14	14.0	14	0.0
3374	14	14.0	14	0.0
4027	14	14.0	14	0.0
4354	13	13.5	14	0.5
4695	14	14.1	15	0.4
5036	14	14.1	15	0.4
5328	13	13.8	15	0.4
10552	14	14.0	14	0.0

Fig.6.1 Cumulative darksignal development pixels over two years in orbit (IRS-1C)



6.2 Response

In order to see any change in the response of photo-diodes, the data of six different intensity levels in calibration cycle are considered module wise. The data is compared after normalising with respect to the channel mean for the orbit and the percentage peak to peak variation is taken for each photo-diode. The distribution of this peak to peak variation among all 2100 photo-diodes is shown in Table 6.4. From this table one can see that there are 14 photo-diodes showing 5% peak to peak deviation in photo-response. Out of these 14 photo-diodes, 10 are among those which have shown increase in dark signal during one year. 648th photo-diode of the array shows very high deviation of 19%.

Table 6.4
Distribution of Pixel Response
variation in IRS-1C

Peak-Peak deviation (%)	Number of pixels in the range
19-20	1
9 - 10	1
7-8	1
6-7	5
5-6	6

7. DISCUSSION

Apart from this SWIR device, Silicon based CCD devices are being used in other wavebands of various cameras of IRS-1C/1D spacecrafts. The past as well as present experience with these silicon based CCD devices do not indicate any abrupt large changes in dark signal as being observed in case of SWIR devices. The main differences of SWIR devices with these Silicon based CCD's are :-

- (a) SWIR device is a hybrid lattice mismatched device
- (b) Operating temperature is lower than the room temperature

In addition, the common factors are:-

- (c) Reverse-biased photo-diode
- (d) Impact of Proton Radiation

The possibility of each of these factors being the cause of observed degradation of the device is discussed below:

(a) Lattice mismatched configuration

As it is already described, the used detector is an InGaAs photo-diode array grown on InP substrate using lattice mismatched technology. This lattice mismatched technology is prone to generate dislocation related crystal defects. If these defects are located at p-n junction or in the space charge region, flow of charge through these defects results in increased leakage current i.e. dark current of the photo-diode. This is as if the band gap of the photo-diode is reduced at the site of the dislocation, in case if InGaAs the band gap is 0.72 eV and if the dislocation is located at p-n junction its activation energy turns out to be 0.52 eV (Ref.1), hence leads to an increased dark current. The number and density of these defects is crystal growth technology dependent and can not evolve with time. Thus, it can not explain the current observation of number of high dark signal pixels increasing with time.

b) Lower operating temperature

Further, the prolonged low temperature operation (-10 °C in case of IRS-1C SWIR device) of the device could result in more stress on the lattice structure leading to generation of lattice defects with time and hence the

evolution of the number of high dark signal pixels with time. But the SWIR device of IRS-1D spacecraft, which is similar to that of IRS-1C, is being operated onboard at 12 °C and shows similar behaviour of temporal evolution of high dark signal pixels. Thus, this hypothesis of low temperature generated stresses producing lattice defects and causing few pixels to develop high dark signal is unlikely.

(c) Reverse-biased Photo-Diode

If dislocation related lattice defect is located at p-n junction or in space charge region, the leakage current (dark signal) of photodiode increases. Large reverse bias voltages will produce larger space charge regions and the possibility of more lattice defects being located in space charge region increases. Thus, in case of temporal development of these defects higher bias voltages increase the possibility of device degradation. A near zero bias operation could be advantageous.

(d) Impact of Particle Radiation

The observed trend of increasing number of high dark signal pixels can be explained by lattice damages caused by particles trapped in the magnetic field of the earth. The radiation belt electron and proton model flux contours in idealised dipole space are shown in Fig. 7.1. This figure shows that in case of low earth orbits like that of IRS-1C spacecraft, protons dominate the particle flux. Further, because of very high probability of being scattered and absorbed while passing through the material before reaching the photo-diodes, very few electrons with very low energy will reach the detector area. Electrons of few hundred KeV energy which are present in low earth orbit radiation belts can not impart sufficient momentum to the atoms of InGaAs to produce dislocation related lattice defects even in case of no material shielding around the active area of photo-diodes. However, Protons follow almost a straight path through material (no scattering because of high mass). In case of low earth orbits, protons of few hundred MeV energy are present in the radiation belts. Aluminium has moderately high stopping power for protons compared to copper. The stopping power of Al shield increases with its thickness up to 4mm and remains almost constant thereafter (Fig.7.2). Thus, about 10 krad(Si) annual proton dosage is certainly there on photo-diodes. This turns out to be about 1E5 MeV per year per pixel (30 μ m \times 30 μ m) energy deposition due to protons. Preliminary calculations show that the energy spectrum of low earth orbit protons, which peaks at about 100 MeV, shifts to a few tens of MeV after passing through the shielding material (4 mm thick Alumina ceramic and 8 mm thick copper cold finger) on the back side of the detector. A proton with such energy is sufficient to dislocate atoms of photo-diode material and produce dislocation related lattice defects that causes high dark signal of the photo-diode.

8 Conclusion

- 1) A study of Short Wave Infrared Linear Array Detector performance in orbit is presented.

- 2) This study indicates abrupt increase in dark signal of some of the individual pixels. There is a monotonic increase with time of such pixels.
- 3) Distribution of such pixels among various modules of the array is uniform.
- 4) The development of such high dark signal is unlikely to be due to lattice mismatch configuration or prolonged low temperature operation.
- 5) Possible impact of proton damage is discussed.

REFERENCES

1. D.Pogany, S.Ababou, G.Guillot, X.Hugon, B.Vilotitch and C.Lenoble, *Solid-State Electronics* 38, 37 (1995)

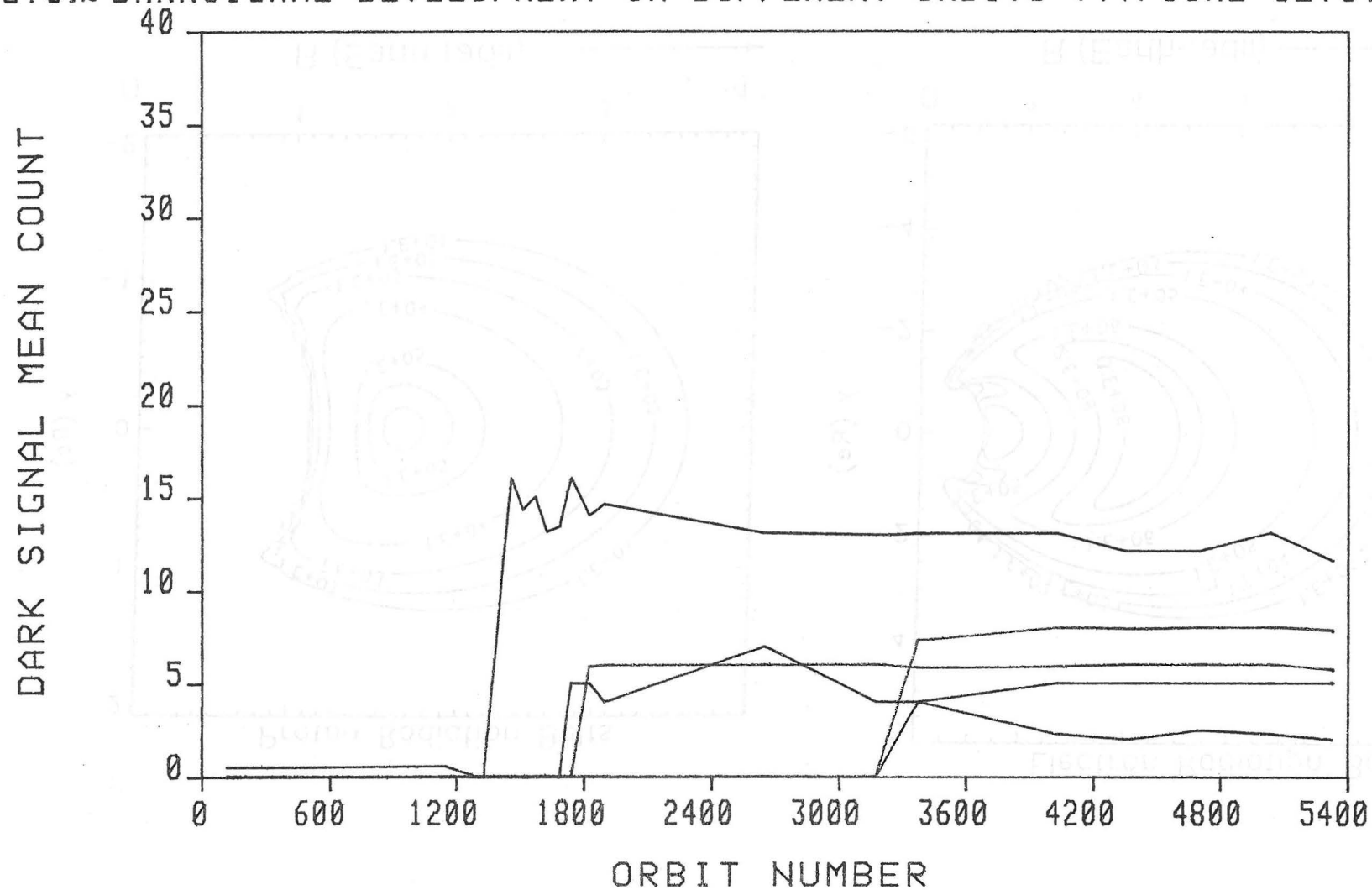
TABLE 6.1D

IRS-1D LISS-3 SWIR DETECTOR PERFORMANCE IN ON-BOARD CALIBRATION MODE IN DIFFERENT ORBITS

Int	Mod	Ch	7Oct97	7Jan98	Int	Mod	Ch	7Oct97	7Jan98
0	1	1	0.1	0.1	4	1	1	15.2	14.4
0	1	2	0.1	0.1	4	1	2	15.3	14.5
0	2	1	0.0	0.0	4	2	1	13.6	12.9
0	2	2	0.1	1.4	4	2	2	13.4	14.1
0	3	1	0.0	0.1	4	3	1	7.5	7.2
0	3	2	0.0	0.0	4	3	2	7.4	7.1
0	4	1	0.2	0.1	4	4	1	15.4	15.1
0	4	2	0.0	0.0	4	4	2	15.3	15.1
0	5	1	0.8	0.9	4	5	1	26.1	25.8
0	5	2	0.9	0.8	4	5	2	25.7	25.2
0	6	1	0.0	0.0	4	6	1	24.4	25.1
0	6	2	0.0	0.1	4	6	2	25.2	25.9
0	7	1	0.0	0.0	4	7	1	13.0	13.4
0	7	2	0.0	0.9	4	7	2	13.5	14.7
1	1	1	7.7	7.4	5	1	1	33.9	33.8
1	1	2	7.8	7.3	5	1	2	33.2	33.1
1	2	1	6.8	6.6	5	2	1	37.3	36.0
1	2	2	6.7	7.7	5	2	2	36.0	35.8
1	3	1	3.8	3.7	5	3	1	32.4	32.1
1	3	2	3.7	3.5	5	3	2	31.2	30.8
1	4	1	7.9	7.7	5	4	1	36.3	36.0
1	4	2	7.6	7.5	5	4	2	35.0	34.7
1	5	1	13.5	13.3	5	5	1	32.6	31.7
1	5	2	13.3	13.1	5	5	2	31.1	30.1
1	6	1	12.3	12.7	5	6	1	43.7	44.3
1	6	2	12.7	13.1	5	6	2	43.3	44.0
1	7	1	6.5	6.7	5	7	1	37.3	37.5
1	7	2	6.7	7.8	5	7	2	37.3	38.0
2	1	1	17.2	17.2	6	1	1	48.8	47.9
2	1	2	16.8	16.7	6	1	2	48.3	47.4
2	2	1	18.9	18.2	6	2	1	50.5	48.7
2	2	2	18.1	18.6	6	2	2	49.5	48.6
2	3	1	16.3	16.3	6	3	1	39.7	39.1
2	3	2	15.7	15.4	6	3	2	38.7	38.0
2	4	1	18.4	18.3	6	4	1	51.4	50.9
2	4	2	17.5	17.4	6	4	2	50.4	49.9
2	5	1	16.8	16.2	6	5	1	57.8	56.5
2	5	2	16.1	15.6	6	5	2	55.9	54.4
2	6	1	22.1	22.4	6	6	1	67.9	69.1
2	6	2	21.9	22.2	6	6	2	68.4	69.7
2	7	1	18.8	18.8	6	7	1	50.3	50.9
2	7	2	18.8	19.6	6	7	2	50.7	51.9
3	1	1	24.7	24.2					
3	1	2	24.3	23.9					
3	2	1	25.5	24.6					
3	2	2	24.9	25.0					
3	3	1	20.0	19.9					
3	3	2	19.4	19.1					
3	4	1	26.0	25.7					
3	4	2	25.3	25.1					
3	5	1	29.6	28.7					
3	5	2	28.5	27.6					
3	6	1	34.2	34.9					
3	6	2	34.4	35.1					
3	7	1	25.3	25.6					
3	7	2	25.5	26.5					

Int - Intensity levels 0 to 6
Mod - Elementary Module number
Ch - Channel (1 for odd and 2 for even pixels)
Values are the channel mean counts

FIG.6.2 DARKSIGNAL DEVELOPMENT IN DIFFERENT ORBITS (TYPICAL SETS)



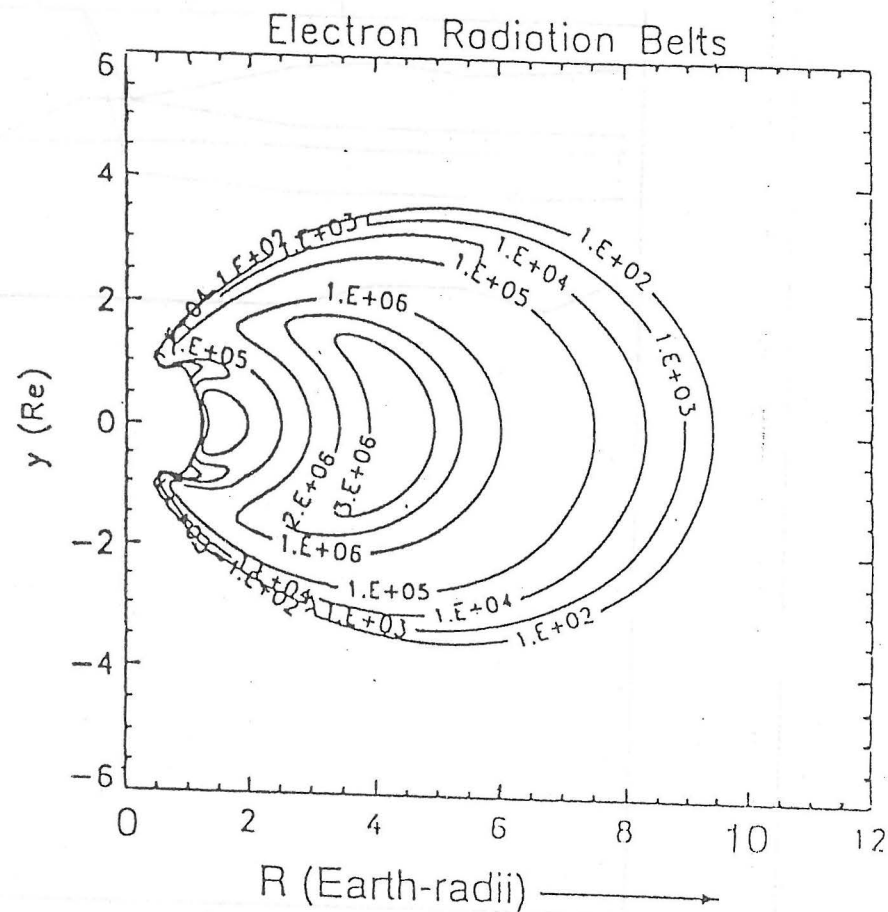
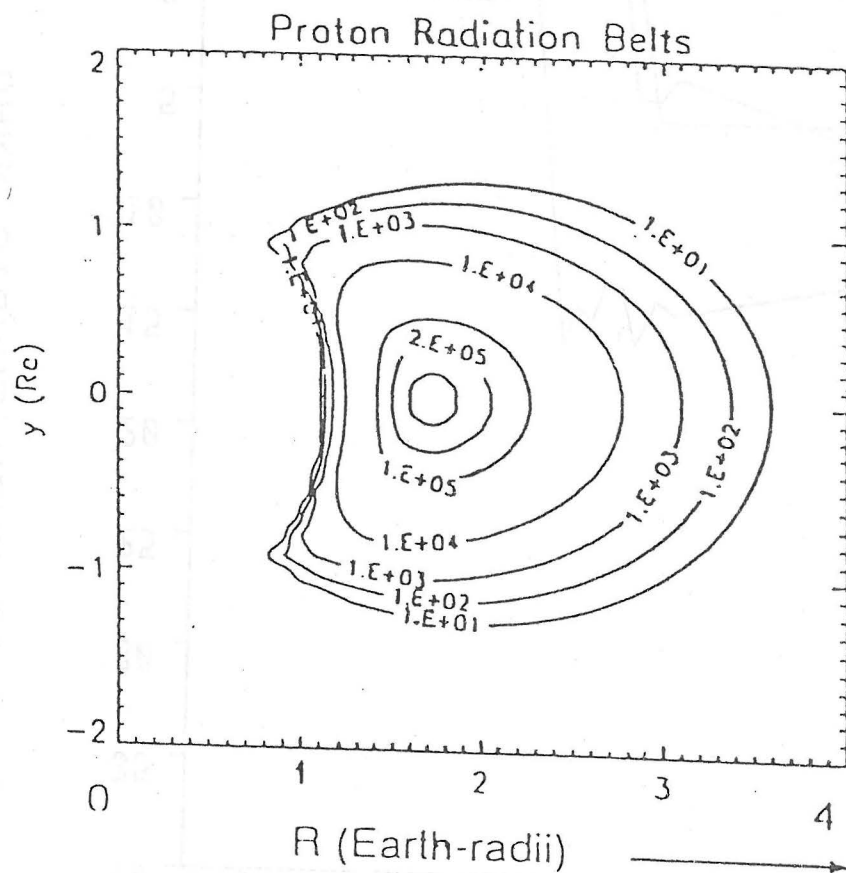


FIG. 7.1

Figure 7.2

LEO 1000 km, SOLAR MIN

